PHYSICAL REVIEW B, VOLUME 65, 121402(R)

Polarized resonant Raman study of isolated single-wall carbon nanotubes: Symmetry selection rules, dipolar and multipolar antenna effects

A. Jorio,[1] A. G. Souza Filho,[1,2] V. W. Brar,[1] A. K. Swan,[3] M. S. Ünlü,[3] B. B. Goldberg,[3,4] A. Righi,[5] J. H. Hafner,[6] C. M. Lieber,[6] R. Saito,[7] G. Dresselhaus,[8] and M. S. Dresselhaus[1,9]

[1]*Department of Physics, Massachusetts Institute of Technology, Cambridge, Massachusetts 02139-4307*

[2]*Departamento de Física, Universidade Federal do Ceará, Fortaleza, CE 60455-760, Brazil*

[3]*Electrical and Computer Engineering Department, Boston University, Boston, Massachusetts 02215*

[4]*Department of Physics, Boston University, Boston, Massachusetts 02215*

[5]*Departamento de Física, Universidade Federal de Minas Gerais, Belo Horizonte, MG 30123-970, Brazil*

[6]*Department of Chemistry, Harvard University, Cambridge, Massachusetts 02138*

[7]*Department of Electronic-Engineering, University of Electro-Communications, Tokyo 182-8585, Japan*

[8]*Francis Bitter Magnet Laboratory, Massachusetts Institute of Technology, Cambridge, Massachusetts 02139-4307*

[9]*Department of Electrical Engineering and Computer Science, Massachusetts Institute of Technology, Cambridge, Massachusetts 02139-4307*

(Received 31 July 2001; revised manuscript received 2 October 2001; published 11 March 2002)

We studied the polarization dependence of the resonance Raman spectra for several different isolated single-wall carbon nanotubes (SWNTs). One isolated SWNT acts as a dipolar antenna, polarized along the tube axis. For light polarized parallel to the tube axis, the strong resonance-effect breaks the symmetry-selection rules, and symmetry-forbidden modes appear in the Raman spectrum. When the light is not polarized parallel to the tube axis, *G*-band mode symmetries can be identified. Unusual *G*-mode intensity behavior is observed when the Raman signal is obtained from more than one SWNT, suggesting a complex multipolar antenna pattern.

DOI: 10.1103/PhysRevB.65.121402 PACS number(s): 78.30.Na, 78.20.Bh, 78.66.Tr, 63.22.+m

Since their first observation in 1993 by Bethune *et al.*[1] and by Iijima and Ichihashi[2] single-wall carbon nanotubes (SWNTs) have been intensively studied for their interesting one-dimensional (1D) physical properties and for their high potential for technological applications.[3,4] Because of their strong electron-phonon coupling under resonance condition and the quantum confinement of the electronic states in this 1D material, resonance Raman spectroscopy has provided a valuable tool for the study of both the vibrational and the electronic properties of SWNTs, first as grown in bundles,[5] and recently also as grown in isolation on a Si/SiO_2 substrate.[6–10] In this work we analyze the dependence of the resonance Raman spectra on the polarization scattering geometry for several different isolated SWNTs. As we discuss here, the polarization dependence of the resonance *G*-band Raman spectra is sensitive to their mode symmetries (A, E_1, and E_2), to the resonant nature of the scattering process, and to the presence of neighboring tubes.

The two important first-order features in the Raman spectra of SWNTs are the radial breathing mode (RBM), with $A(A_{1g})$ symmetry and the tangential *G* band, composed of six modes, two of each of the symmetries: $A(A_{1g})$, $E_1(E_{1g})$, and $E_2(E_{2g})$.[3,5] So far, most of the work using polarized resonance Raman spectroscopy on aligned SWNT samples reported a simple intensity dependence for the Raman signal, where all the modes exhibit a maximum when the light is polarized along the tube axis, and is strongly suppressed when the light (either incident or scattered) is polarized perpendicular to the tube axis.[11–13] These polarization effects are due to the resonant nature of the Raman scattering process in SWNTs, as predicted by Ajiki and Ando.[14] A symmetry-selection study of the *G*-band modes was already reported in the polarized resonance Raman spectra of aligned SWNT *bundles* at $E_{\text{laser}}=2.41$ eV excitation, with a SWNT broad diameter distribution peaked at $d_t=1.85$ nm, showing that the *G*-band profile for *semiconducting* SWNTs can be deconvolved into four components with the following symmetry assignments: 1549 $\text{cm}^{-1}(E_2)$, 1567 $\text{cm}^{-1}(A+E_1)$, 1590 $\text{cm}^{-1}(A+E_1)$, and 1607 $\text{cm}^{-1}(E_2)$.[15]

In the present work we show, by studying *isolated* SWNTs, that the polarization behavior of the Raman modes exhibits a much more complicated behavior than the simple dipolar antenna effect that has been considered previously.[11–13] A symmetry-selection analysis[15,16] can, in fact, be carried out when light is not polarized parallel to the tube axis. Furthermore, we show that the presence of neighboring isolated SWNTs modify the simple dipolar antenna behavior of a single isolated SWNT.

The *isolated* SWNTs were prepared by a chemical vapor-deposition method on a Si/SiO_2 substrate containing nanometer-sized iron-catalyst particles.[6] This procedure is more reliable than previously reported methods of sample preparation for single nanotube spectroscopy,[11,13] since only isolated tubes are grown and no SWNT bundles are formed.[17] Atomic-force microscopy images show that the sample has SWNTs with diameters d_t ranging from 1 to 3 nm, a very low SWNT density, containing only ~ 40 nanotubes in a 100 μm^2 area, and providing good spatial isolation between the SWNTs. Very few of them ($<10\%$) are found to be close enough to each other to be illuminated at the same time in one laser spot (~ 1 μm). Raman spectra from isolated SWNTs resonant with the incident laser light [514.5 nm ($E_{\text{laser}}=2.41$ eV) from an Ar ion laser] were obtained using a single monochromator Renishaw spectrom-

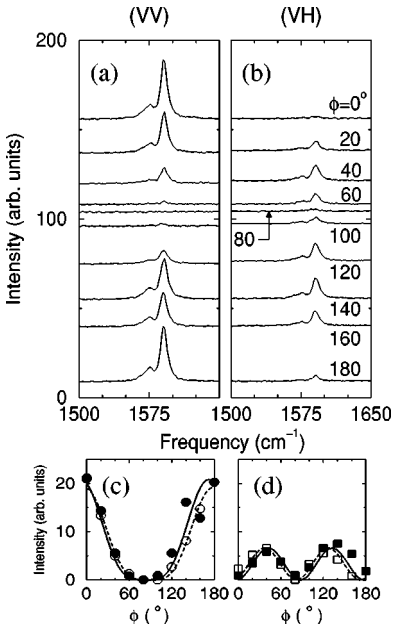

FIG. 1. (a) and (b) show the VV and VH *G*-band Raman spectra from one light spot on the sample, taken with different angles ϕ (see text). The filled symbols in (c) and (d) show the VV and VH *G*-band integrated intensity (Lorentzian fit) for the light spot shown in (a) and (b). Open symbols show similar behavior for a resonant SWNT in another light spot. The solid/dashed curves show a fit to the solid/open data points with the functions (c) $\cos^4(\phi+\Delta\phi)$ and (d) $\sin^2(\phi+\Delta\phi)\cos^2(\phi+\Delta\phi)$, with $\Delta\phi=7.9°$ for both solid curves and $\Delta\phi=1.7°$ for both dashed curves.

eter, equipped with a notch filter and a charge-coupled device (CCD) detector. A set of lenses put in the laser path expands the beam diameter to benefit from the maximum available numerical aperture, hence, getting the highest spatial resolution. The Raman spectra were collected in a backscattering configuration by a microscope using a 50× objective. To avoid polarization effects related to the spectrometer optics, the polarization studies were performed using a $\lambda/2$ plate situated close to the sample (at the enlarged laser beam), to rotate both the incident and backscattered light. A fixed polarizer was used to analyze the scattered light polarized parallel to the incident-light polarization (VV configuration). To obtain the VH signal (incident and scattered-light polarized perpendicular to each other), the scattered light was rotated by another $\lambda/2$ plate, keeping the same scattered-light polarization direction in the grating and in the CCD.

Figures 1(a) and 1(b) display, respectively, the VV and VH *G*-band Raman spectra taken from one light spot on the sample where a SWNT resonant with E_{laser} was found. The angle between the nanotube axis and the incident-light polarization is denoted by ϕ. The dependence of the *G*-band integrated intensity on the angle ϕ is shown in Figs. 1(c) VV and 1(d) VH with filled symbols. Open symbols show the ϕ angular dependence of the VV and VH resonant Raman signal for a different SWNT sitting at another light spot on the substrate. Both SWNTs exhibit the same ϕ polarization dependence, and the same ϕ dependence is also found for the $A(A_{1g})$ RBM (not shown in the figure). The points in Figs. 1(c) and 1(d) can be fit well with $\cos^4(\phi+\Delta\phi)$ (VV) and $\sin^2(\phi+\Delta\phi)\cos^2(\phi+\Delta\phi)$ (VH) functions, that account for the incident and scattered electric-field components along the axis of a perfectly aligned SWNT (see Ref. 12). The nanotube axis direction ($\phi=0°$) was found by turning the $\lambda/2$ plate to obtain the maximum signal, according to the depolarization effect.[14] $\Delta\phi$ accounts for the error in the experimental setting of $\phi=0°$. We obtained $\Delta\phi=7.9°$ for the solid data points corresponding to the SWNT in Figs. 1(a) and 1(b), and we obtained $\Delta\phi=1.7°$ for the open-symbol data points in (c) and (d). This procedure can be used to find the nanotube orientation on a surface to high accuracy.

The results shown in Figs. 1(a) and 1(b) are in agreement with previous works,[11–13] and with polarization measurements performed on several other isolated SWNTs on the same Si/SiO_2 substrate as was used for Fig. 1 (not shown here). It is important to note that previous results on nonaligned SWNT bundles indicate that the antenna effect is stronger for metallic SWNTs than for semiconducting SWNTs.[16,18,19] From the various features (RBM, *G* band, *D* band, G' band) in the Raman spectra of isolated SWNTs, we can identify the atomic and electronic structure of a SWNT that is resonant with a given laser excitation energy E_{laser}.[6–10] By analyzing the different isolated SWNTs observed in this work, we conclude that the antenna effect is strongly operative for SWNTs resonant with various E_{ii} transitions (we measured semiconducting SWNTs with $i=2$ to 5), for the resonance occurring with either the incident or scattered photons, and for SWNTs up to relatively large diameters ($d_t>2.0$ nm).

It is noteworthy that according to group theory, the ZZ polarized spectra (incident and scattered light polarized along the tube axis, equivalent to the VV spectra at $\phi=0°$ or at 180° in Fig. 1) should exhibit only $A(A_{1g})$ modes. However, all the *G*-band modes are observed, indicating that the strong-resonance effect breaks the symmetry-selection rules. When the polarization direction of the light is turned with respect to the tube axis, the polarization effect is suppressed, and the symmetry-selection rules could then be elucidated. This result is shown in Fig. 2 for another light spot on the sample, where the antenna effect for the *G*-band spectra is shown in Fig. 2(a) for $\phi=0°$ to $\phi=80°$. The inset to Fig. 2(a) shows the RBM at 174 cm^{-1}. Figure 2(b) shows all the spectra in Fig. 2(a) normalized according to the highest intensity peak at 1592 cm^{-1}. A different intensity behavior for different modes is clearly observed. Figure 2(c) shows the VV and VH spectra for $\phi=80°$. According to group theory,[15] the VV spectrum should be dominated by two $A(A_g)$ and two $E_2(E_{2g})$ modes, the E_2 modes being close to its maximum contribution.[20] The VH spectrum should be dominated by two $E_1(E_{1g})$ modes. We can thus make the following symmetry assignments: one $E_2(E_{2g})$ mode appears at 1555 cm^{-1}; two $E_1(E_{1g})$ modes appear at 1566 and 1592 cm^{-1}; and two $A(A_{1g})$ modes appear at 1578 and 1592 cm^{-1}. These results are in excellent agreement with theoretical predictions with respect to the frequency ordering of the different symmetry modes,[20,21] and also in good agreement with previously reported experimental results for

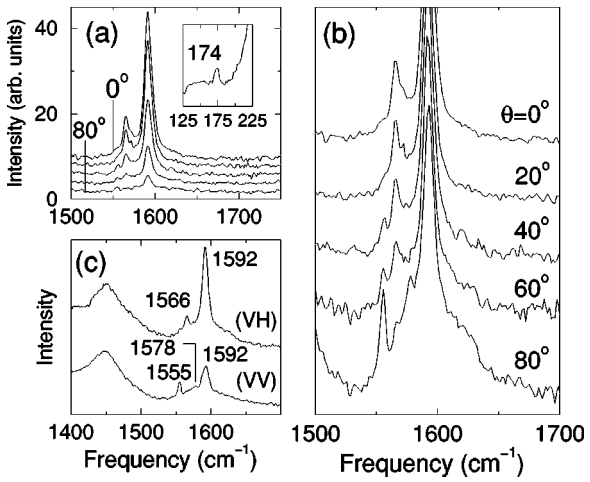

FIG. 2. Raman spectra for a different light-spot position on the Si/SiO_2 substrate than for Fig. 1. (a) shows the antenna effect for the *G*-band spectra, for $\phi=0°$ to $\phi=80°$. The inset to (a) shows the RBM feature at 174 cm^{-1}, which characterizes the tube diameter $d_t=1.43$ nm.[6] (b) shows the spectra in (a), but normalized to the highest intensity peak at 1592 cm^{-1}. (c) shows the VV and VH spectra for $\phi=80°$. The mode frequencies are all displayed in cm^{-1}.

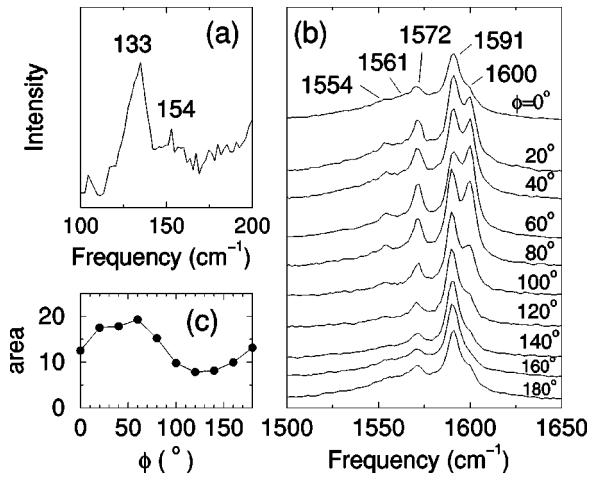

FIG. 3. (a) Raman spectrum of the RBMs for one light spot on the sample. (b) The ϕ dependence of the *G*-band Raman spectra in the same spot as (a), with the *G*-band mode frequencies displayed (cm^{-1}). (c) The ϕ dependence of the *G*-band integrated intensities (arb. units) in (b).

aligned SWNT bundles.[15,16] It is important to notice that the small spectral features in Fig. 2(c) have a very low intensity and, therefore, a long accumulation time is necessary to observe the modes experimentally. However, the results are reproducible and were observed in more than one isolated SWNT (results not shown here).

Although the antenna effect seems to be the general behavior for one isolated SWNT, we, however, find resonant SWNTs for a small number of light spots that exhibit unusual intensity behavior for the several *G*-band modes, and do not exhibit a strong suppression of the Raman signal for light polarized perpendicular to the nanotube axis. In these cases, such as in the example shown in Fig. 3, we observe two peaks in the RBM region [Fig. 3(a)], indicative of two resonant SWNTs in the same light spot, i.e., distant from each other by less than the wavelength of the light. The *G*-band spectra in Fig. 3(b) exhibit a complicated and unusual ϕ angular dependence that cannot be understood considering the dipolar antenna effect and group-theory predictions: (i) the intensity for the 1572 cm^{-1} and 1591 cm^{-1} peaks are practically constant for all values of ϕ; (ii) there is an unusually intense peak at 1600 cm^{-1} with a strong ϕ dependence, being a maximum when the total Raman integrated intensity [Fig. 3(c)] is a maximum. The results presented in Fig. 3 suggest that the two superimposed dipole fields from two nanotubes at different origins and with different relative orientations modify the simple dipolar antenna pattern of one single isolated SWNT, resulting in a complex multipole antenna pattern. The SWNTs in Fig. 3 can be tentatively assigned as the (23,1) and (18,4) that, according to Ref. 6, should have RBMs, respectively, at 133 and 154 cm^{-1}, as observed, and E_{44}^S at 2.36 and 2.39 eV, respectively. The very close values of E_{44}^S for these tubes suggest the possibility of strong coupling in forming the local field multipolar antenna pattern. The identification of this unusual polarization behavior with the presence of more than one SWNT within the same light spot is confirmed by measuring the polarization behavior of SWNT samples with a larger density of tubes in the Si/SiO_2 substrate. In such larger density samples, unusual behavior of this kind is observed more often. Furthermore, these results can explain how in aligned multiwall carbon nanotubes[22] and in semiconducting SWNTs in bundles,[15,16] the polarization behavior was observed to be consistent with bond-polarization theory.[20] The depolarization effects can be suppressed by the electronic field from other graphitic layers or by neighboring SWNTs.

In summary, we showed that a single isolated SWNT acts as a dipole antenna, with the emission of Raman scattered light being strongly suppressed when the incident or scattered light is polarized perpendicular to the nanotube axis, in agreement with previous studies.[11–13] From the several features in the Raman spectra of the isolated SWNTs we can identify structural and electronic properties,[6–10] and we found that the antenna effect is observed independent of the resonant electronic transition E_{ii}, whether the resonance occurs with the incident or scattered photon, and the antenna effect seems to be effective even for relatively large diameter SWNTs ($d_t>2$ nm).

For light polarized along the tube axis, the strong resonance effect breaks the symmetry-selection rules and symmetry-forbidden modes can be observed. When the light is not polarized parallel to the tube axis, *G*-band mode symmetries are identified by polarization selection rules. The results are in good agreement with theoretical predictions[20,21] and experimental observations on SWNT bundles.[15,16]

We also report on the suppression of the antenna effect in light spots where the Raman signal was obtained from more than one SWNT, suggesting that the two superimposed dipole fields from different origins and orientations modify the simple dipolar antenna pattern of an isolated SWNT. The unusual intensity polarization behavior of the different

G-band symmetry modes provide evidence for this multipolar antenna pattern. It is important to note that different unusual intensity polarization behaviors were observed for different light spots with two resonant SWNTs. This result indicates that different nanotubes with different spatial arrangements (different origin and axes orientations) give different multipolar antenna patterns. To clarify this rich polarization behavior, new experiments need to be performed by using sufficiently advanced technology to manipulate the relative position between two neighboring SWNTs.

We acknowledge Ge. G. Samsonidze, K. Kneipp, and M. A. Pimenta for critical readings of the manuscript. A.J./A.G.S.F./A.R. acknowledge support from the Brazilian agencies CNPq/CAPES/FAPEMIG. The MIT authors acknowledge support under NSF Grant Nos. DMR 01-16042, INT 98-15744, and INT 00-00408. R.S. acknowledges a Grant in Aid (No. 13440091) from the Ministry of Education, Japan. The experimental work was performed at the Photonics Center, Boston University (BU). BU authors acknowledge support from Renishaw Inc. and DARPA HERETIC Program.

[1] D.S. Bethune, C.H. Kiang, M.S. de Vries, G. Gorman, R. Savoy, J. Vazquez, and R. Beyers, Nature (London) **363**, 605 (1993).

[2] S. Iijima and T. Ichihashi, Nature (London) **363**, 603 (1993).

[3] R. Saito, G. Dresselhaus, and M.S. Dresselhaus, *Physical Properties of Carbon Nanotubes* (Imperial College Press, London, 1998).

[4] M.S. Dresselhaus, G. Dresselhaus, and Ph. Avouris, *Carbon Nanotubes: Synthesis, Structure, Properties and Applications*, Springer Series in Topics in Applied Physics Vol. 80 (Springer-Verlag, Berlin, 2001).

[5] M.S. Dresselhaus and P.C. Eklund, Adv. Phys. **49**, 705 (2000).

[6] A. Jorio, R. Saito, J.H. Hafner, C.M. Lieber, M. Hunter, T. McClure, G. Dresselhaus, and M.S. Dresselhaus, Phys. Rev. Lett. **86**, 1118 (2001).

[7] M.A. Pimenta, A. Jorio, S.D.M. Brown, A.G. Souza Filho, G. Dresselhaus, J.H. Hafner, C.M. Lieber, R. Saito, and M.S. Dresselhaus, Phys. Rev. B **64**, 041401 (2001).

[8] A.G. Souza Filho, A. Jorio, J.H. Hafner, C.M. Lieber, R. Saito, M.A. Pimenta, G. Dresselhaus, and M.S. Dresselhaus, Phys. Rev. B **63**, R241404 (2001).

[9] A.G. Souza Filho, A. Jorio, G. Dresselhaus, M.S. Dresselhaus, R. Saito, Anna K. Swan, M.S. Ünlü, B.B. Goldberg, J.H. Hafner, C.M. Lieber, and M.A. Pimenta, Phys. Rev. B **65**, 035404 (2002).

[10] A. Jorio, A.G. Souza Filho, G. Dresselhaus, M.S. Dresselhaus, A.K. Swan, B. Goldberg, M.S. Ünlü, M.A. Pimenta, J.H. Hafner, C.M. Lieber, and R. Saito, Phys. Rev. B (to be published).

[11] G.S. Duesberg, I. Loa, M. Burghard, K. Syassen, and S. Roth, Phys. Rev. Lett. **85**, 5436 (2000).

[12] J. Hwang, H.H. Gommans, A. Ugawa, H. Tashiro, R. Haggenmueller, K.I. Winey, J.E. Fischer, D.B. Tanner, and A.G. Rinzler, Phys. Rev. B **62**, R13 310 (2000).

[13] Z. Yu and L.E. Brus, J. Phys. Chem. B **105**, 1123 (2001).

[14] H. Ajiki and T. Ando, Physica B **201**, 349 (1994).

[15] A. Jorio, G. Dresselhaus, M.S. Dresselhaus, M. Souza, M.S.S. Dantas, M.A. Pimenta, A.M. Rao, R. Saito, C. Liu, and H.M. Cheng, Phys. Rev. Lett. **85**, 2617 (2000).

[16] C. Fantini, M.A. Pimenta, M.S.S. Dantas, D. Ugarte, A.M. Rao, A. Jorio, G. Dresselhaus, and M.S. Dresselhaus, Phys. Rev. B **63**, 161405 (2001).

[17] J.H. Hafner, C.L. Cheung, T.H. Oosterkamp, and C.M. Lieber, J. Phys. Chem. B **105**, 743 (2001).

[18] A. Jorio, S.D.M. Brown, G. Dresselhaus, M.S. Dresselhaus, M.A. Pimenta, R. Saito, A.M. Rao, and K. Kneipp, in *Nanotubes and Related Materials*, Boston, 2000, edited by A. M. Rao, Mater. Res. Soc. Symp. Proc. (Materials Research Society, Pittsburgh, PA, 2000).

[19] K. Kneipp, A. Jorio, H. Kneipp, S.D.M. Brown, K. Shafer, J. Motz, R. Saito, G. Dresselhaus, and M.S. Dresselhaus, Phys. Rev. B **63**, 081401 (2001).

[20] R. Saito, T. Takeya, T. Kimura, G. Dresselhaus, and M.S. Dresselhaus, Phys. Rev. B **57**, 4145 (1998).

[21] R. Saito, A. Jorio, J.H. Hafner, C.M. Lieber, M. Hunter, T. McClure, G. Dresselhaus, and M.S. Dresselhaus, Phys. Rev. B **64**, 085312 (2001).

[22] A.M. Rao, A. Jorio, M.A. Pimenta, M.S.S. Dantas, R. Saito, G. Dresselhaus, and M.S. Dresselhaus, Phys. Rev. Lett. **84**, 1820 (2000).